

PREFERENTIAL FILTERING AND GRAVITY ANOMALY SEPERATION USING GRAVITY RECOVERY AND INTERIOR LABORATORY (GRAIL) DATA. N. R. Maksim¹, J. Biddle², and J. M. Hurtado, Jr.³, ^{1,2,3}The University of Texas at El Paso, Department of Geological Sciences, 500 West University Avenue, El Paso TX 79968, ¹nrhodes@miners.utep.edu, ²jbiddle@miners.utep.edu, ³jhurtado@utep.edu

Introduction: Understanding the lunar gravity field can provide fundamental information about lunar internal structure, bulk composition, heat flow, and the duration of volcanism and tectonism. We aim to utilize the gravity field from the Gravity Recovery and Interior Laboratory (GRAIL) mission to reconstruct the history of lunar volcanic history. The high-resolution GRAIL gravity maps show that over 98% of the Moon's gravity anomalies are associated with topography, and only 2% of the gravity anomalies represent subsurface structures [1]. The subsurface of the Moon has been highly affected by impacts that have not only changed the topography but have also produced impact melts that altered subsurface densities and porosities [1]. For this reason, even after the free-air correction, the Moon's free-air anomaly map still mostly reflects high-frequency gravitational anomalies due to impacts [1]. In order to retrieve gravity anomalies that represent interior structure rather than surficial features, we performed a preferential filtering on the free-air anomaly map derived from GRAIL lunar gravity model GL0660A. We then constructed a 2D inversion model to visualize potential intrusive bodies in the lunar crust.

Gravity Data: High-resolution measurements of the lunar gravity field were recently made by the GRAIL mission [1]. The available Radio Science Digital Map Product (RSDMAP) data products are derived from the GL0660A GRAIL lunar gravity model [1]. GL0660A is a degree and order 660 spherical harmonic model (truncated to degree and order 320) [1], and it is available from the Planetary Data System (PDS) LGRS RDR archive. The free-air gravity anomaly map has a resolution of 4 pixel/degree (~7.6 km/pixel on a reference sphere with semi-major-axis radius of 1,738.0 km) [1]. Each pixel gives free-air gravity anomaly in milligals (mGal).

Preferential Filtering and Gravity Anomaly Separation: In the spatial domain, the total free-air gravity anomaly, $g_{fa}(x,y)$, is the sum of gravitational anomalies originating from the deep subsurface, $g_d(x,y)$, and gravitational anomalies originating from the shallow subsurface, $g_s(x,y)$ [2,3]:

$$g_{fa}(x,y) = g_d(x,y) + g_s(x,y) \quad (1).$$

Similarly, in the frequency domain, the Fourier power spectrum (P) of the total free-air gravity signal is the sum of the radially averaged power spectra of subsurface (P_i) components [4]:

$$P = P_{d1} + P_{d2} + \dots + P_{d_i} + P_{s1} + P_{s2} + \dots + P_{s_i} \quad (2).$$

The power spectrum of the gravity signal due to a subsurface layer is an exponential function [5,6]:

$$P = se^{-2kh} \quad (3),$$

where h is the depth to the subsurface layer, k is the angular, or radial, frequency of its power spectrum, and the constant s is the strength, or intensity, of the gravitational signal associated with that layer [5,6]. Combining Eqs. (2) and (3) yields [4]:

$$P = s_1 e^{-2k_1 h_1} + s_2 e^{-2k_2 h_2} + \dots + s_n e^{-2k_n h_n} \quad (4).$$

We use a preferential filtering method to eliminate high-frequency anomalies associated with surficial features. The preferential filtering method is similar to frequency-domain Wiener filtering [7,9]. We use this method to filter the free-air gravity anomaly data at a specific bandwidth in order to selectively retrieve the gravity signal associated with a specific depth [7,8,9]. The Wiener preferential filtering operator we use is of the form [7,8]:

$$W_{pfi} = \frac{P_i}{P_{i,cat}} \quad (5),$$

where P_i is the power spectrum of the gravity signal of subsurface layer i and $P_{i,cat}$ is the calculated ideal power spectrum of subsurface layer i .

To perform the preferential filtering, we imported the GL0660A free-air gravity anomaly data into MATLAB. We transformed the data into the frequency domain and calculated the radially-averaged power spectrum (P) using the `raPsd2d` command. This calculates and plots P versus radial frequency, k , on a logarithmic scale. P can be divided into several components (P_1, P_2, \dots, P_n), each representing the power of an individual subsurface layer (Eqs. (2) and (4)). We apply a piece-wise linearization (using the `lsq_lut` command) to fit straight-line segments to each power spectrum component (P_i). These fits provide estimates of $P_{i,cat}$ for each layer. We use this to determine W_{pfi} in Eq. (5).

From the piece-wise best-fit segments, h and s for each subsurface layer can be calculated [7]. To obtain h we use [8]:

$$h = \frac{P(k_1) - P(k_2)}{4\pi(k_1 - k_2)} \quad (6),$$

where k_1 and k_2 are the start and end of radial frequencies of a given spectral segment and $P(k_1)$ and $P(k_2)$ are the values of the radially averaged power spectra at the start and end of a given spectral segment [7,8]. To filter the gravity signal from target layer i , we apply the W_{pfi} calculated for the target layer to our gravity data in the frequency domain [7,9]. We then apply an inverse Fourier transformation to the result to yield the filtered free air gravity anomaly of target layer i in the spatial domain.

2D Inversion Modeling: To resolve the internal structure of the lunar crust, we built an inverse model

from the filtered free-air gravity anomaly data using *Geosoft Oasis Montage v. 6.2*. To build the model, we created a 2-dimensional model of the Moon's crustal structures. Because geological information (e.g. seismic data, boreholes, magnetic data, etc.) for the Moon are limited, our model was only constrained by surface geological features such as the distribution of mare and highlands lithologies [11,12]. It includes the following density values: for mafic intrusions, we use the density of mare basalt ($3,150 \text{ kg/m}^3$) [1,11,12]; for the lunar crust we use an average density of $2,560 \text{ kg/m}^3$ [1,11]; and, for two large plutonic bodies interpreted near Mare Imbrium, we use a density of $2,770 \text{ kg/m}^3$ [10].

Results: Our analysis reveals five layers at depths of 0.17, 0.42, -0.94, -3.64 and -4.93 km (positive "depths" refer to features above the geoid). We are particularly interested in the subsurface layer at 3.64 km depth because it has the highest signal strength ($2.43 \times 10^3 \text{ gal}^2 \text{ Hz}^{-1}$; the others are $0.01\text{--}0.1 \times 10^3 \text{ gal}^2 \text{ Hz}^{-1}$). The filtered gravity anomaly map is smoother, with fewer short- to intermediate-wavelength features, than the non-filtered free-air anomaly (Fig. 1a). Fig. 1b shows that the preferentially filtered gravity anomaly map has (mostly positive) magnitudes between -10 and 45 mGal. We constructed our 2D inversion model at a depth of 3.64 km along this transect across latitude 37° N (Fig. 1c). The RMS misfit between the inversion model and the filtered data is small (1.019%).

Conclusion: We successfully filtered and separated the gravity anomaly of a target layer at 3.64 km depth from the total free-air gravity anomaly using the preferential filtering method. Our 2-D inversion model also successfully provided us some good insight to the Moon's volcanic history including zones of intrusions and possible mascons bodies. We model the strongest anomalies in the filtered data, which originate from a depth of 3.64 km along latitude 37° N . The model suggests four 14–25 km mafic intrusions: two underneath Oceanus Procellarum and two near Cleomedes (Fig. 1c). These mafic intrusions are associated with the locations of cryptomaria [13] and a high gravity gradient area that has been interpreted by previous workers to be the frozen remnants of lava-filled rifts and the underlying feeder dikes [14]. Our model also suggests two moderate-density ($2,770 \text{ kg/m}^3$) bodies, each about 90–145 km in width, underneath Mare Imbrium and Mare Serenitatis (Fig. 1c). The low-density contrast (110 kg/m^3) between these bodies and the surrounding crustal material indicates that they are not associated with mare basalt. In our model, these bodies produce positive gravity anomalies of 10–40 mGal, which is consistent with previous work on mascon basins [15]. However, because they are at a depth of 3.64 km, these anomalous bodies may be too shallow to be mascons [16]. An alternative possibility is that the bodies maybe remnants of the Moon's lower crust.

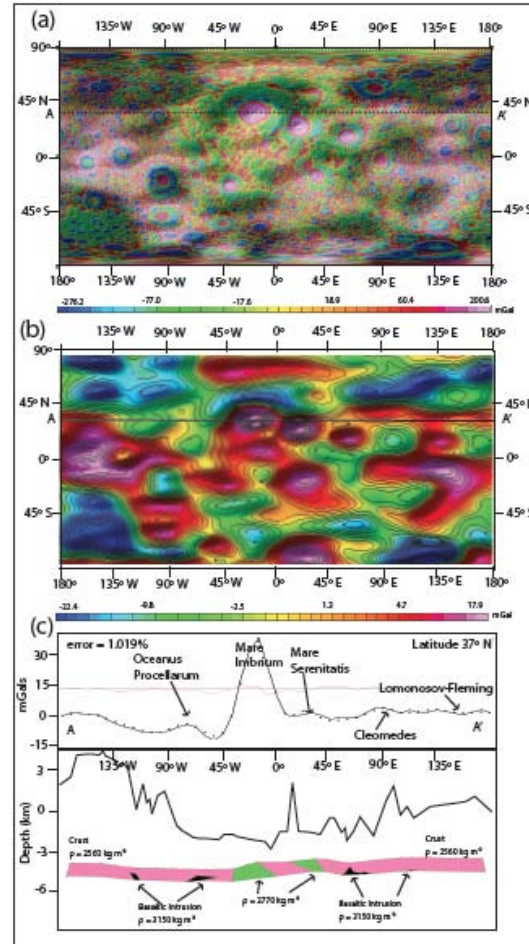


Fig. 1. (a) The preferentially-filtered (3.64 km depth), free-air gravity anomaly (in grayscale) is overlain on the (unfiltered) GL0660A free-air gravity anomaly map of the Moon (in color). (b) Contoured map of the preferentially-filtered (3.64 km depth) free-air gravity anomaly. (c, top) Comparison between the modeled free-air gravity anomaly (black line) and the filtered free-air gravity anomaly data (black dots). (c, bottom) 2D inversion model of lunar crustal structure and topographic profile with 266x vertical exaggeration at a depth of 3.64 km at latitude 37° N [transect A-A' in (a) and (b)]. Black line is the topographic profile.

References: [1] Zuber et al. (2013) *Science*, 339, 668-671; [2] Milsom (2007) *John Wiley and Sons Inc, USA*; [3] Nettleton (1957) *Geophys.*, 19 (1), 1-22; [4] Powlowski (1994) *Geophys.*, 55 (5), 69-76; [5] Naidu (1968) *Geophys.*, 33, 337-345; [6] Dampney (1969) *Geophys.*, 34 (5), 39-53; [7] Guo et al., (2013) *Comput Geosci.*, 51, 247-254; [8] Spector and Grant (1970) *Geophys.*, 35 (2), 293-302; [9] Wiener (1949) *John Wiley and Sons Inc, USA*; [10] Phillips (2007) *US Geological Survey*, 1355; [11] Wieczorek et al. (2006) *Rev Mineral Geochem.*, 60 (1), 221-364; [12] Kiefer et al. (2012) *LPSC abstract*, 43; [13] Whitten and Head (2015) *Icarus*, 247, 150-171; [14] Andrews-Hanna et al. (2014) *Nature*, 514, 68-71; [15] Miljković et al. (2015) *Earth Planet. Sci. Lett.*, 409, 243-251; [16] Wieczorek and Phillips (1998) *J. Geophys. Res.*, 103, 1715-1724.